*Neuroscience* 117 (2003) 293–303

# ASSOCIATION OF ATP SYNTHASE α-CHAIN WITH NEUROFIBRILLARY DEGENERATION IN ALZHEIMER'S DISEASE

**N. SERGEANT,[a] A. WATTEZ,[a] M. GALVÁN-VALENCIA,[b] A. GHESTEM,[a] J.-P. DAVID,[a] J. LEMOINE,[c] P.-E. SAUTIÉRE,[d] J. DACHARY,[e] J.-P. MAZAT,[e] J.-C. MICHALSKI,[c] J. VELOURS,[f] R. MENA-LÓPEZ[b] AND A. DELACOURTE[a]***

[a]*Unite INSERM 422, 1, Place de Verdun, Lille Cedex 59045, France*

[b]*Departamento de Fisiología Biofísica y Neurociencias, CINVESTAV-IPN, P.O. Box 14-740, 07000, México D.F.*

[c]*CNRS UMR 8576, UFR de Biologie, Bât. C9, 59655 Villeneuve d'Ascq, France*

[d]*Laboratoire d'Endocrinologie des Annélides, UPRESA 8017, Bât. SN3, 59655 Villeneuve d'Ascq, France*

[e]*INSERM EMI 9929, Université Victor Segalen Bordeaux 2, 146, rue Léo Saignat, 33076 Bordeaux cedex, France*

[f]*CNRS UMR 5095, Institut de Biochimie et Génétique Cellulaires, 1, rue Camille Saint Saens, 33077 Bordeaux cedex, France*

**Abstract—Amyloid deposits and neurofibrillary tangles (NFT) are the two hallmarks that characterize Alzheimer's disease (AD). In order to find the molecular partners of these degenerating processes, we have developed antibodies against insoluble AD brain lesions. One clone, named AD46, detects only NFT. Biochemical and histochemistry analyses demonstrate that the labeled protein accumulating in the cytosol of Alzheimer degenerating neurons is the α-chain of the ATP synthase. The cytosolic accumulation of the α-chain of ATP synthase is observed even at early stages of neurofibrillary degenerating process. It is specifically observed in degenerating neurons, either alone or tightly associated with aggregates of tau proteins, suggesting that it is a new molecular event related to neurodegeneration.**

**Overall, our results strongly suggest the implication of the α-chain of ATP synthase in neurofibrillary degeneration of AD that is illustrated by the cytosolic accumulation of this mitochondrial protein, which belongs to the mitochondrial respiratory system. This regulatory subunit of the respiratory complex V of mitochondria is thus a potential target for therapeutic and diagnostic strategies. © 2003 Published by Elsevier Science Ltd on behalf of IBRO.**

**Key words: neurodegeneration, oxidative phosphorylation, proteomic, microtubule-associated tau protein, paired helical filament, neurofibrillary tangle.**

*Corresponding author. Tel: +33-3-20-62-2077; fax: +33-3-20-62-2079.
E-mail address: delacourte@lille.inserm.fr (A. Delacourte).

*Abbreviations:* AD, Alzheimer's disease; APP, amyloid precursor protein; EDTA, ethylenediaminetetraacetic acid; EGTA, ethylene glycol-bis aminoethyl ether tetraacetic acid; i.p., immunoprecipitation; NFT, neurofibrillary tangles; NEPHGE, non-equilibrium pH gradient gel electrophoresis; NSE, neuron-specific enolase; OXPHOS, oxidative phosphorylation; PHF, paired helical filaments; pI, isoelectric point; SDS, sodium dodecyl sulfate; PAGE, polyacrylamide gel electrophoresis; w/v, weight/volume; 2-D, two-dimensional.

Amyloid deposits and neurofibrillary tangles (NFT) are the two neuropathological features of Alzheimer's disease (AD) (Braak and Braak, 1991; Delacourte et al., 2002). Amyloid β-peptides are the major components of amyloid deposits (Glenner and Wong, 1984). They result from the catabolism of a type I transmembrane glycoprotein named APP (amyloid precursor protein) (Kang et al., 1987). NFT are bundles of paired helical filaments (PHF) composed essentially of modified microtubule-associated tau proteins, named pathological tau proteins or PHF-tau (Brion et al., 1985; Delacourte and Defossez, 1986; Grundke-Iqbal et al., 1986; Nukina and Ihara, 1986; Wood et al., 1986).

Many additional molecules co-aggregate with amyloid deposits and PHF (e.g. apolipoprotein E, heparan sulfate proteoglycans, growth factors, protein kinases) (Permanne et al., 1995; Buee, 1999; Hensley et al., 1999; Cho et al., 2001), some of which could play a pivotal role in degenerating processes. However, it remains difficult to know if such molecules contribute to the aggregating processes or if their aggregation is a consequence. Previous biochemical analyses have shown that many of those molecules are co-purified with the insoluble material of AD brain tissue (Permanne et al., 1995). We have used this insoluble material to develop monoclonal antibodies using an *in vitro* immunization system. The clones were selected for their ability to react with AD brain lesions. Antigens were characterized using proteomic, and confirmed with specific antibodies against the identified proteins. One protein more closely related to neurodegeneration was investigated further, including its colocalisation with PHF and NFT, its co-purification with PHF-tau and conversely, PHF-tau were visualized following immunoprecipitation of the identified protein. This protein belongs to the complex V of respiratory system of mitochondria. Our molecular investigation strongly supports the implication of this mitochondrial protein in the neurodegenerative process of AD.

## EXPERIMENTAL PROCEDURES

### Patients

All of the brain autopsy materials used in the present study were from our brain bank. The AD and control cases were described earlier (Delacourte et al., 1999, 2002). After death, one hemisphere was deep-frozen for biochemical analyses and the other hemisphere was formalin-fixed for both neuropathological examination and histochemistry. AD46 ascite fluid was produced and it was systematically used in parallel of AD2 labeling (see paragraph concerning antibodies), in a prospective histochemical study performed upon more than 130 cases, including non-demented and AD patients as described in Delacourte et al. (1999). Biochemical analyses have been performed on the most representative controls (five cases) and AD patients (10 cases).

0306-4522/03$30.00+0.00 © 2003 Published by Elsevier Science Ltd on behalf of IBRO.
doi:10.1016/S0306-4522(02)00747-9

### Antibodies

The monoclonal antibody AD46 was obtained using an *in vitro* immunization kit (Immune System, Bristol, UK) with semi-purified formic acid-insoluble material obtained from the brain tissue of an AD patient. The immunogene was prepared as described earlier (Permanne et al., 1995). The immunized splenocytes, obtained according to the manufacturer's instructions, were fused with myeloma cells. The screening of hybridoma supernatants was performed by histochemistry on AD and control brain tissue sections. The positive clones selected were produced as ascite fluid. Additional antibodies were used. The γ-enolase or neuron-specific enolase (NSE) antibody, named 1C1, was developed in our laboratory (Sergeant et al., 2002). The β-actin antibody A5441 was from Sigma (Saint Quentin Fallavier, France). The ATP synthase α-chain antiserum was raised against the yeast protein. It reacts with ATP synthase α-chain of other organisms including human (Lefebvre-Legendre et al., 2001). AD2 antibody detects pathological tau proteins in AD brain tissue homogenates. It is raised against the phosphorylated serines 396 and 404 of the longest human tau isoform (Buee-Scherrer et al., 1996). Tau-Cter antiserum, raised against the carboxy-terminal part of tau proteins, recognizes phosphorylated and non-phosphorylated tau proteins (Sergeant et al., 2001).

### Brain tissue sample preparation

Brain tissue samples were homogenized using a Teflon potter homogenizer in 10-mM Tris–HCl pH 6.8 solution (1/10 weight/volume [w/v]) containing a cocktail of protease inhibitors (Complete EDTA-free protease inhibitor tablets, Roche Molecular Biochemicals). The homogenate was centrifuged at 100,000×*g* during 1 h at 4 °C, the supernatant (S1) was collected and the pellet (P1) was homogenized in the starting buffer added with 0.5% Triton X-100. Supernatant S2 was obtained after centrifugation at 100,000×*g* during 1 h. The pellet (P2) was homogenized in the starting buffer added with 2% of Triton X-100 and the supernatant (S3) was obtained following centrifugation (100,000×*g*, 1 h). The final pellet (P4) was homogenized in Laemmli sample buffer (Laemmli, 1970). One-half of the supernatants (S1–S3) were used for Western blotting, the second half of the supernatants was kept for two-dimensional (2-D) gel electrophoresis. The protein concentration was determined using the BCA protein assay kit (Pierce, Perbio Science, Bezons, France), in accordance with the manufacturer's instructions.

### PHF preparation and immunoprecipitation

PHF made of bundles of tau proteins were prepared according to the method described by Greenberg and Davies (1990) and modified by Goedert et al. (1992). Briefly, brain tissue was homogenized in 10 volumes of sucrose buffer containing 10-mM Tris–HCl pH 7.4, 800-mM NaCl, 1-mM EGTA and 10% sucrose at 4 °C, using a Teflon potter. The resulting homogenate was centrifuged at 20,000×*g* during 30 min at 4 °C. The supernatant was collected; the pellet was homogenized in sucrose buffer followed by an additional centrifugation. Supernatants were combined and added with a final concentration of 1% (w/v) of *N*-laurylsarcosinate and gently mixed at ambient temperature for 1 h. The sarcosyl-homogenate was spun at 100,000×*g* during 1 h. The resulting pellet was resuspended in sodium dodecyl sulfate (SDS) buffer (10-mM Tris–HCl pH 6.8, 2% SDS, 10-mM DTT, 10% glycerol), sonicated and boiled 10 min at 100 °C.

For immunoprecipitation (i.p.) experiments, the brain tissue was homogenized in 10 volumes of Tris-buffered saline (10-mM Tris–HCl pH 7.4, 150-mM NaCl) and spun at 27,200×*g* for 30 min at 4 °C, according to the method described by Vincent and Davies (1992). The resulting supernatant was used for i.p. Briefly, the supernatant was clarified with 10 μl of Ultralink Immobilized Protein A/G Plus (Pierce) during 30 min at 4 °C while shaking and protein A/G beads were discarded following centrifugation. The resulting supernatant was incubated with 10 μl of ATP synthase α-chain antiserum or 5 μl of AD46 antibody and gently mixed overnight at 4 °C. Ten microliters of Protein A/G beads were then added and incubated for an additional 30 min at 4 °C. The beads were collected following centrifugation and rinsed three times with homogenization buffer. Immunoprecipitated complexes were resuspended in SDS buffer and incubated at 60 °C during 5 min and centrifuged using Handee spin cup columns (Pierce) in accordance with the manufacturer's instructions.

### Mono- and two-dimensional gel electrophoresis

An equal amount of protein was loaded onto 8–16% polyacrylamide gradient gel electrophoresis (SDS-PAGE). 2-D gel electrophoresis was performed as described earlier (Sergeant et al., 1997) and non-equilibrium pH gradient gel electrophoresis (NEPHGE) was performed following the procedure of O'Farrell et al. (1977). 2-D gels were followed by Western blotting or stained with Coomassie Blue Brilliant for the digestion of the protein inside the gel piece and mass spectrometric analyses.

### Polypeptide in gel trypsin digestion and mass spectrometry

After Coomassie Blue staining, gels were extensively rinsed in water. Protein spots were processed essentially as described by Andersen and Mann (2000). Peptide masses were acquired with a matrix-assisted laser desorption ionization–time-of-flight spectrometer (Voyager II, Perseptive, Applied Biosystem, USA) (Lemoine et al., 1996).

### Western blot

Polyacrylamide gels were transferred onto 0.45-μm pore size nitrocellulose membranes (Hybond ECL, Amersham) for 90 min at 0.8 mA/cm$^2$ using an LKB Multiphor II Nova blot system (Pharmacia). Blotted proteins were reversibly stained with Ponceau Red 2R in order to check the quality of the resolution and to calibrate the 2-D gels isoelectric points using the Carbamylyte calibration kit (Pharmacia) and apparent molecular weights using the broad-range molecular-weight standards (BioRad). Western blotting was performed as described earlier (Sergeant et al., 1997).

### Histochemistry, electron microscopy and laser-scanning confocal microscopy

Histochemistry and electron microscopy were performed following the procedure described by Reig et al. (1995). Immunofluorescence labeling and laser-scanning confocal microscopy procedure is described elsewhere (Mena et al., 1996; Garcia-Sierra et al., 2000).

## RESULTS

One clone, named AD46 clearly stained NFT on AD brain slices (Fig. 1A, B) while a background staining of the neuropil and neurons was observed on control brain tissue section (Fig. 1C). AD46 staining was also very similar to that obtained with AD2 antibody (Fig. 1A), which specifically detects NFT in numerous neurodegenerating disorders (for review see Buee et al., 2000). At the electron microscopy level, AD46 staining colocalized with PHF (Fig. 1D) suggesting that the antibody recognizes microtubule-associated tau proteins. Western blots on total brain tissue

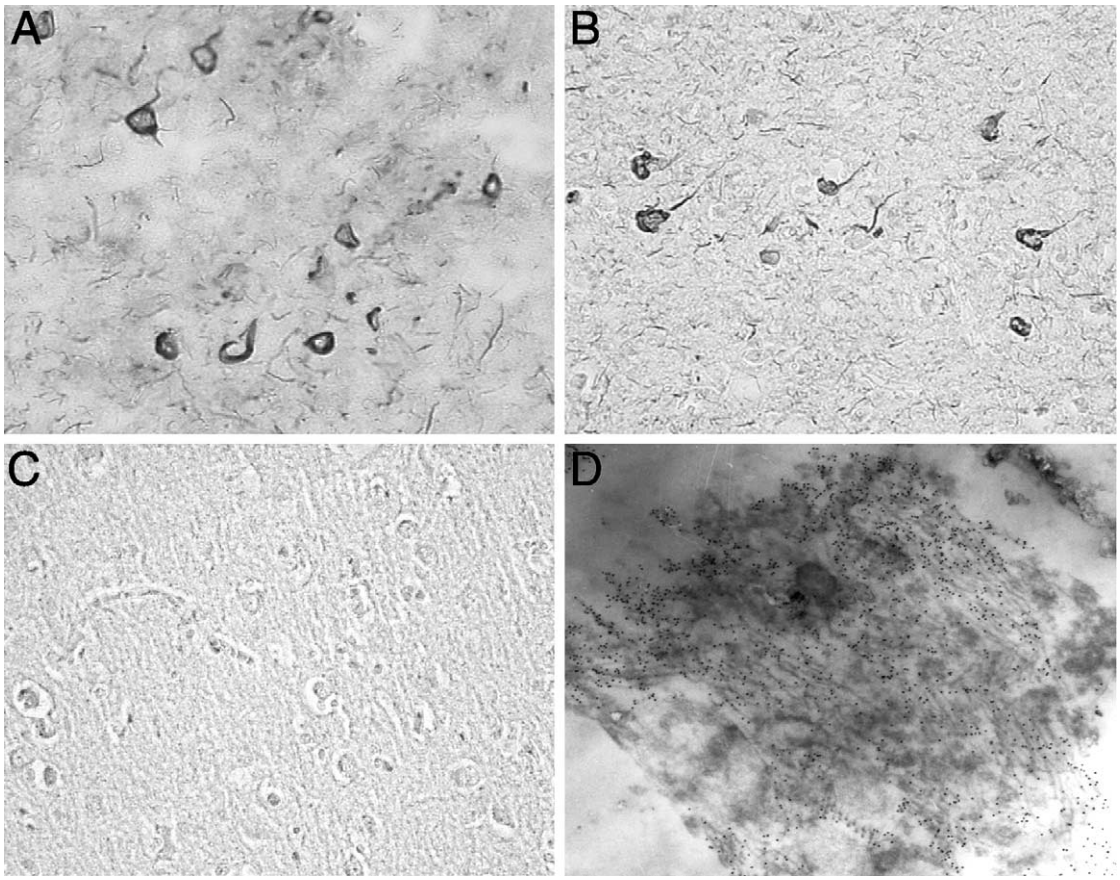


**Fig. 1.** Histochemical and electron microscopy characterization of Alzheimer's disease (AD) 46 antibody. (A) AD2 antibody was used as positive control for the labeling of neurofibrillary tangles (NFT) on AD brain tissue slices. (B) Among all hybridoma supernatants tested the clone AD46 strongly labeled numerous NFT of AD. (C) Light background staining of the neuropil and the soma of neurons was observed with AD46 antibody on control brain-tissue slice. (D) Immunogold labeling was observed by electronic microscopy. AD46 strongly labeled paired helical filaments in degenerating neurons of AD.

homogenates were performed. AD46 antibody detected three bands at 42, 47 and 55 kDa that are distinct from pathological tau as shown by AD2 labeling on an AD brain-tissue homogenate (Fig. 2A). AD46 staining pattern was similar between control and AD total brain-tissue homogenates. Thus, the three polypeptides could correspond to different variants either of the same protein or to multiple proteins. Sub-cloning of AD46 hybridoma failed to modify the immunoreactivity of the antibody (not shown).

Two-dimensional gel electrophoresis followed by AD46 labeling showed four main isovariants (Fig. 2B). The isovariants, visible on Coomassie-stained gels, were isolated and analyzed by mass spectrometry. Intriguingly, the four isovariants corresponded to four distinct proteins (Table 1): the actin cytoplasmic ($\beta$-actin: 42 kDa, isoelectric point [pI] of 5.5), the NSE or $\gamma$-enolase and the $\alpha$-enolase (47 kDa, pI of 5.0 and pI of 7.0, respectively), and the $\alpha$-chain of ATP synthase. Multiple sequence alignment investigation failed to demonstrate any sequence homology or motif that could be shared by the four proteins.

Antibodies against each of the proteins were used to confirm the biochemical identification and histochemistry analyses were performed on control and AD brain tissue. The $\beta$-actin and enolases antibodies detected identical isovariants on 2-D gels as those labeled by AD46 antibody. Thus, 1C1 antibody specific for NSE (Sergeant et al., 2002) detected a single spot and catabolic products of NSE (Fig. 2B). Non-equilibrium pH gradient gel electrophoresis is more adapted to separate basic proteins (O'Farrell et al., 1977). It was used to analyze ATP synthase $\alpha$-chain (Fig. 3A). AD46 labeled a major spot at 55 kDa and pI 8.2 that was also detected with the ATP synthase $\alpha$-chain antiserum (Fig. 3A). AD46 specifically detected the ATP synthase $\alpha$-chain in mitochondria preparation of rat brain, demonstrating the strong immunoreactivity of AD46 antibody for this protein (Fig. 3B). Moreover, in contrast to $\beta$-actin and enolases antibodies, the ATP synthase $\alpha$-chain antiserum strongly labeled NFT on AD brain tissue sections whereas in control brain a background staining of the neuropil and the soma of neurons was observed (Fig. 3C). This result demonstrates that ATP synthase $\alpha$-chain accumulates in the cytosol of degenerating neurons in AD.

As shown by many investigators, the aggregation of tau proteins in degenerating neurons is associated with the change of their solubility properties (Goedert et al., 1992).

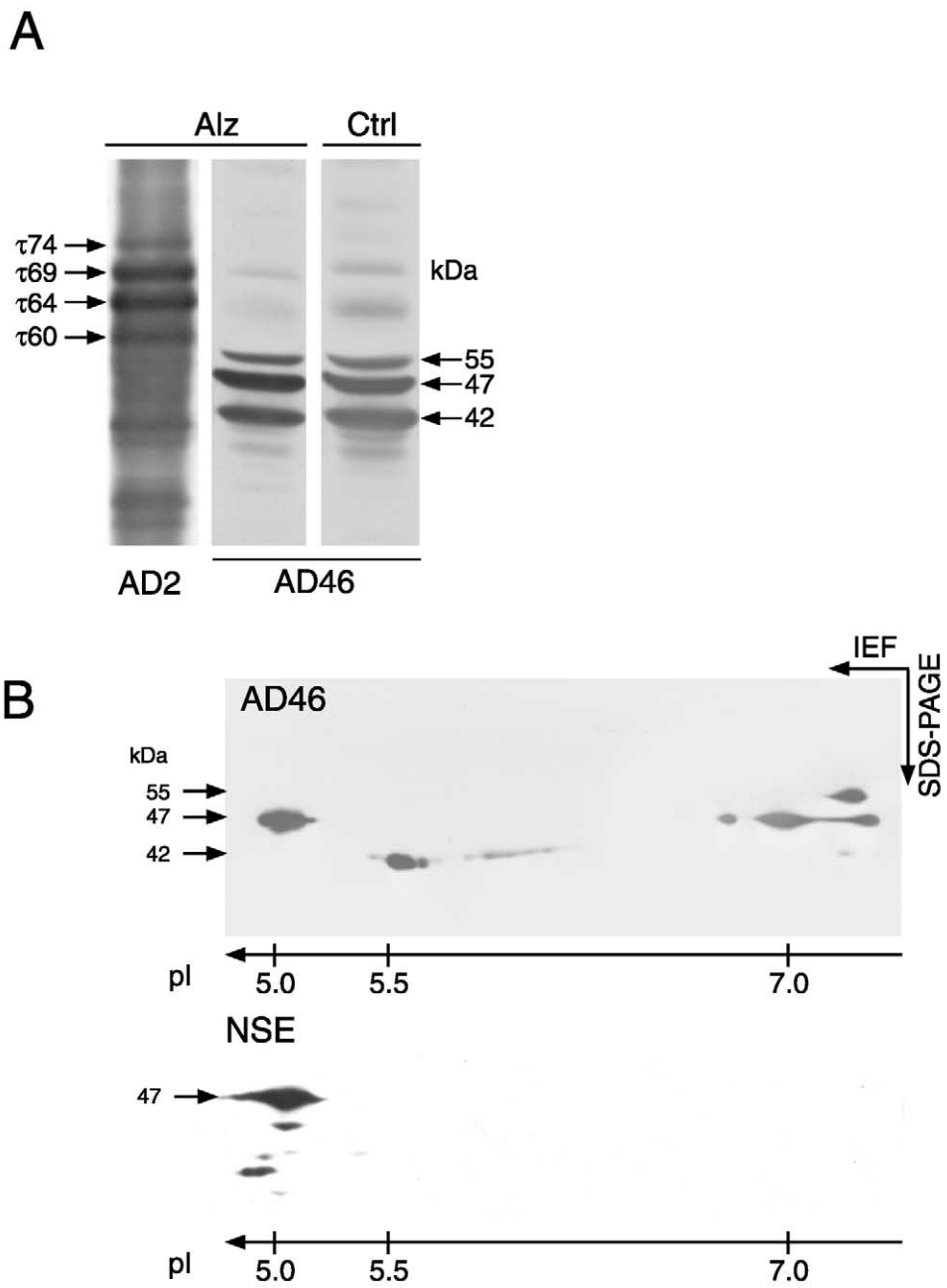


**Fig. 2.** Comparative analyses of the polypeptides detected by Alzheimer's disease (AD) 46 antibody in AD and control. (A) An AD and a control brain-tissue homogenate (indicated at the top by Alz and Ctrl, respectively) were loaded on 8–16% gradient sodium dodecyl sulfate-polyacrylamide gel electrophoresis. Proteins were transferred on nitrocellulose followed by immunostaining with AD2 and AD46 antibody. AD2 detected the typical triplet of pathological tau proteins at 60, 64, 69 kDa and a minor 74-kDa pathological tau component (AD2 lane, pathological tau proteins are indicated by arrows). Three polypeptides at 42, 47 and 55 kDa (indicated on the right by arrows) were detected in the AD brain-tissue homogenate and the Ctrl brain-tissue homogenate. No significant difference of the AD46 immunolabeling pattern is observed between the AD and Ctrl brain-tissue homogenate. A similar experiment was performed with 10 AD and 10 Ctrl brain-tissue homogenate. The three polypeptides detected by AD46 were in similar amounts (data not shown). (B) Brain-tissue proteins from control and AD patient were separated by two-dimensional (2-D) gel electrophoresis followed by Western blotting with AD46 and neuron-specific enolase (NSE) antibodies. The 2-D Western blot profiles were similar between AD and Ctrl samples, and shown for a control brain-tissue homogenate. A major spot is observed at the isoelectric point (pI) of 5.5 for the 42-kDa polypeptides. At 47 kDa two major spots at pI 5.0 and 7.0 are detected by AD46 antibody, and a single basic spot is stained at 55 kDa. 1C1 monoclonal antibody, specific for NSE stains a major isovariant at 47 kDa and pI 5.0. Lower-molecular-weight staining corresponds to catabolic products of NSE. The isoelectric points are indicated on the abscissa axis.

The change of solubility of the proteins detected by AD46 antibody was investigated. β-actin and enolases are cytosolic proteins that should be detected in the most soluble fractions. ATP synthase α-chain is a subunit of the inner membrane of mitochondria that was expected to be found in less soluble fractions. As shown on Fig. 4 the enolases

**Table 1.** Mass spectrometric protein identification[a]

| Protein | Organism | Reference number | MW/pI theo. | MW/pI obs. | Id. |
|---|---|---|---|---|---|
| Actin cytoplasmic | Human | P02570 | 41.6/5.29 | 42/5.5 | MPF/WB |
| γ-Enolase (EC 4.2.1.11) | Human | P09104 | 47.1/4.94 | 47/5.0 | MPF/WB |
| α-Enolase (EC 4.2.1.11) | Human | P06733 | 47.0/6.99 | 47/7.0 | MPF |
| ATP synthase α-chain (EC 3.6.1.34) | Human | P25705 | 55.2/8.28 | 55/8.2 | MPF/WB |

[a] Immunolabeled Alzheimer's disease (AD) 46 spots were isolated on Coomassie-stained two-dimensional gels and gel-trypsin digestion was performed. The peptides obtained were analyzed by mass spectrometry and proteins were identified on Swiss-protein database. The protein name, the organism and reference number, according to the numbering of Swiss-Protein databank, is indicated in the corresponding columns. The theoretical and observed molecular weights (MW) and isoelectric points (pI) are given. All the proteins have been identified (Id. column) by mass-peptide fingerprint (MPF) and the identity or three out of four proteins has been confirmed using specific antibody and Western blotting (WB, e.g. on Fig. 3).

(47-kDa band) were detected by AD46 in the most soluble fractions (Fig. 4A: fractions S1 and S2). The β-actin (42-kDa band) was detected in all fractions whereas the ATP synthase α-chain (55-kDa band) was only observed in the fractions containing detergents (Fig. 4A: from fraction S2 to P4). An insoluble pool of ATP synthase α-chain was observed in P4 fraction in control and AD cases (Fig. 4A: fraction P4). The pattern of protein solubility was not altered by postmortem delay. Indeed, similar results were observed for protein fractions obtained from a biopsy-

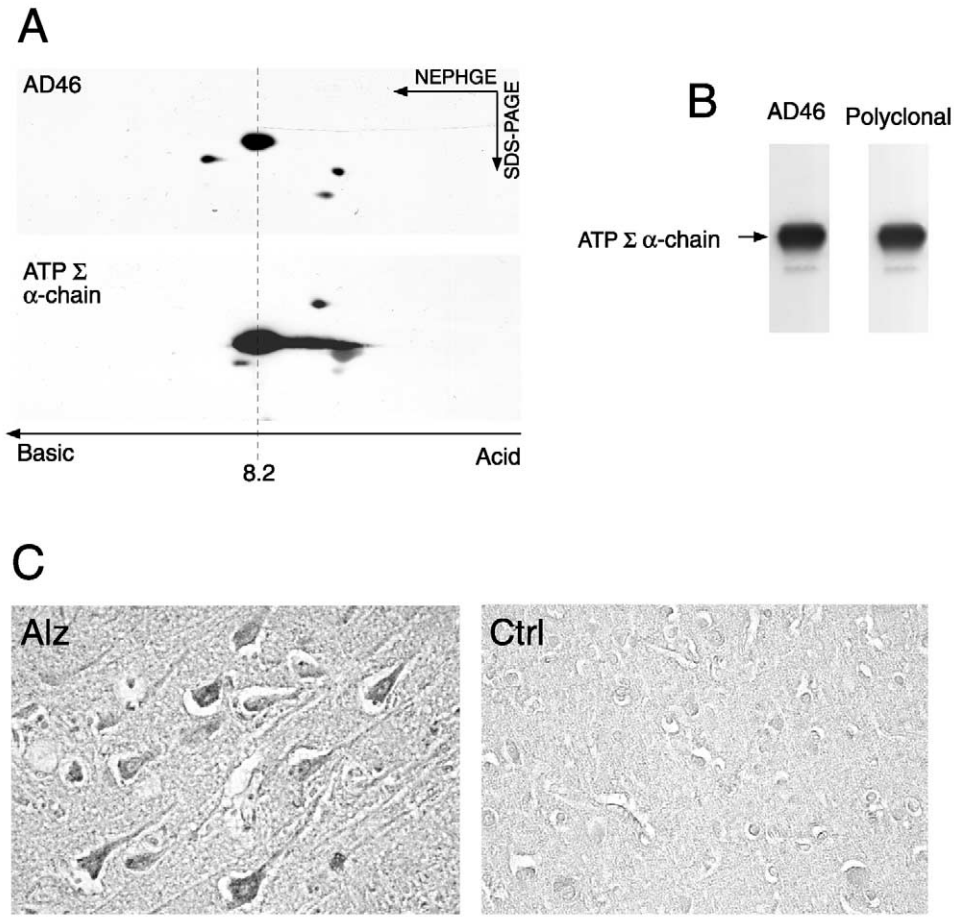


**Fig. 3.** Immunochemical characterization of ATP synthase α-chain and immunostaining of neurofibrillary degeneration. (A) The identity of the proteins was verified using specific antibodies. As an example, the polypeptide at 55 kDa was identified by mass spectrometry as the ATP synthase α-chain. Using non-equilibrium pH gradient gel electrophoresis followed by Western blotting with an ATP synthase α-chain antiserum (ATP Σ α-chain), the identical polypeptide was detected with Alzheimer's disease (AD) 46 antibody and the antiserum. (B) The specificity of both AD46 antibody and ATP synthase α-chain antiserum has been tested on a preparation of mitochondria obtained from a rat brain. A single band at 55 kDa (indicated by an arrow) is detected by AD46 antibody (AD46 lane) and the ATP synthase α-chain antiserum (polyclonal lane). (C) The antibodies against the actin, neuron-specific enolase and ATP synthase α-chain antiserum were also used for histochemistry on control (Ctrl) and AD brain-tissue (Alz) slices. The antiserum against the ATP synthase α-chain stained numerous neurofibrillary tangles (NFT) on AD brain-tissue slices whereas a light background staining was observed on control brain tissue. Both anti-actin and anti-neuron-specific enolase failed to detect NFT in AD or neurons in control brain-tissue sections, respectively (data not shown).

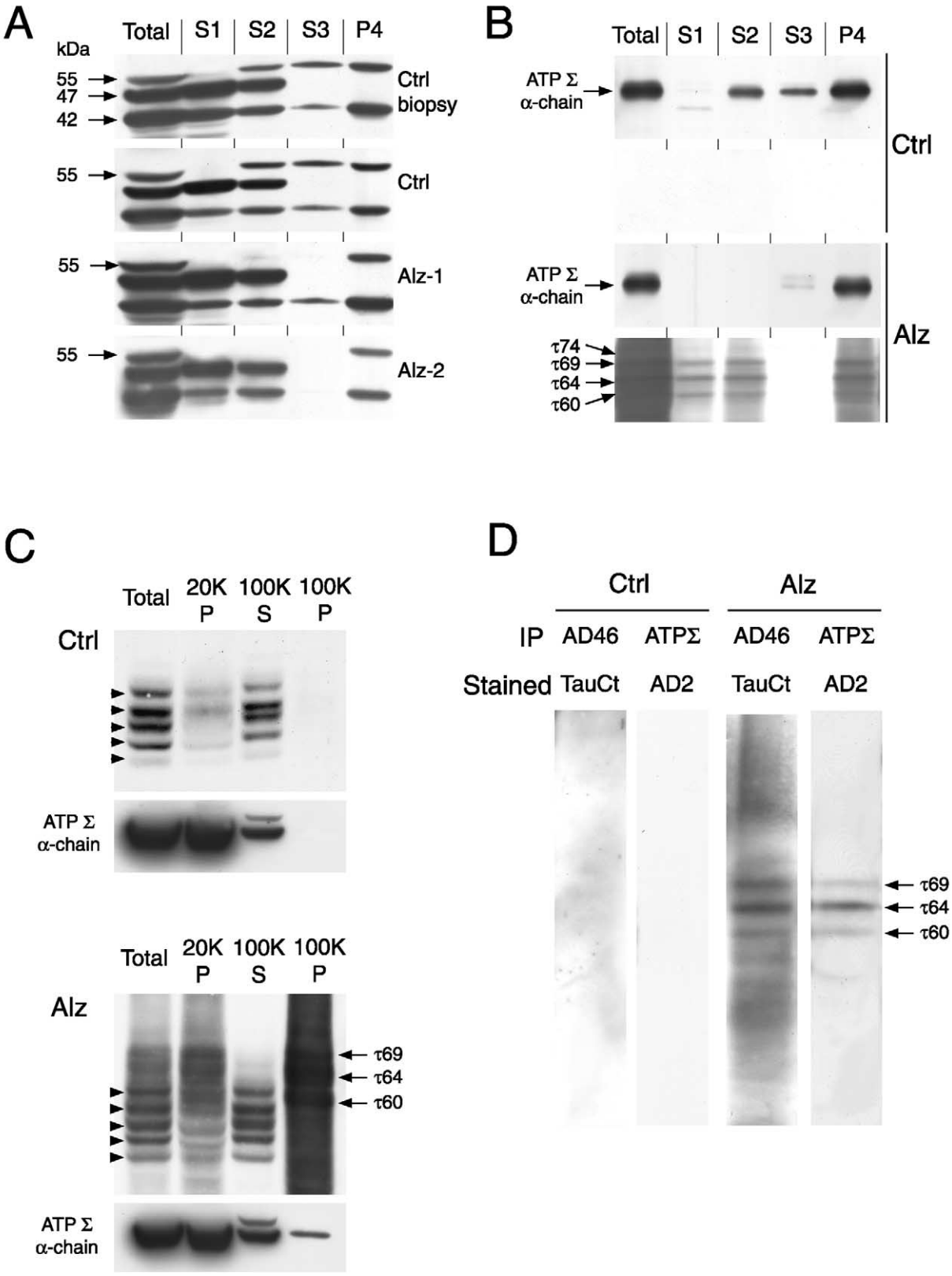
A
Total
S1
S2
S3
P4
kDa
55
47
42
Ctrl
biopsy
55
Ctrl
55
Alz-1
55
Alz-2
B
Total
S1
S2
S3
P4
ATP Σ
α-chain
Ctrl
ATP Σ
α-chain
Alz
τ74
τ69
τ64
τ60
C
Total
20K P
100K S
100K P
Ctrl
ATP Σ
α-chain
Total
20K P
100K S
100K P
Alz
τ69
τ64
τ60
ATP Σ
α-chain
D
Ctrl
Alz
IP
AD46
ATPΣ
AD46
ATPΣ
Stained
TauCt
AD2
TauCt
AD2
τ69
τ64
τ60

**Fig. 4.**

derived control brain tissue (Fig. 4A: biopsy). In contrast, in AD protein fractionation, the staining of ATP synthase α-chain was restricted to the detergent-insoluble fraction P4 (Fig. 4A: fraction P4) whereas in biopsy-derived and autopsy-derived control brain-tissue fractionation, the ATP synthase α-chain was also observed in the detergent-soluble fractions S2 and S3. Identical results were obtained with ATP synthase α-chain antiserum, showing the disappearance of immunoreactivity in AD fractions S2 and S3 (Fig. 4B). The loss of ATP synthase α-chain staining was associated with the presence of pathological tau proteins (Fig. 4B). Thus, PHF were enriched in the sarcosyl-insoluble fraction (Fig. 4C) (Greenberg et al., 1990; Goedert et al., 1992). The experiment was performed in control and AD cases, and tau proteins were stained with a carboxy-terminal tau antiserum. Aggregates of tau protein were recovered in the sarcosyl pellet in AD (Fig. 4C, lane 100K P). The ATP synthase α-chain was also observed in the sarcosyl pellet of the AD case but not in the control case. However, larger amount of ATP synthase α-chain was observed in the sarcosyl supernatant suggesting that the association of ATP synthase α-chain with PHF is reversible. I.p. with both AD46 and ATP synthase α-chain antibodies pulled down pathological tau proteins of AD brain tissue but not normal tau of control (Fig. 4D).

The association of ATP synthase α-chain with pathological tau was further investigated by laser-scanning confocal microscopy. A double labeling was performed with AD46 antibody and tau antiserum or ATP synthase α-chain antiserum and AD2 (Fig. 5). Most of NFT detected by tau antiserum were also labeled by AD46, but tau and AD46 staining did not fully overlap (Fig. 5A). Moreover, some NFT were detected only by tau antiserum whereas others were only detected with AD46 antibody (Fig. 5B). Double staining with AD2 and ATP synthase α-chain showed an overlapping of the staining (Fig. 5C, D). Both antibodies detected NFT and neuropil threads (Fig. 5E). Moreover, AD2 staining showed a typical staining of a neuritic plaque (Fig. 5C) and the degenerating processes were also stained by ATP synthase α-chain (Fig. 5D).

## DISCUSSION

An *in vitro* immunization kit was used to develop monoclonal antibodies in order to find additional molecular partners of the aggregating processes of AD, that are likely to be found in the most insoluble material of the brain tissue of AD patients (Permanne et al., 1995). One clone, AD46, recognized NFT at light microscopy level and decorated PHF at the electron microscopy level, thus suggesting an additional antibody against tau protein. Surprisingly, the biochemical characterization of polypeptides detected by AD46 showed no sequence identity with tau proteins. The proteomic characterization demonstrated the immunoreactivity of AD46 with four individual proteins including the β-actin, the α- and γ-enolase and the ATP synthase α-chain. The reactivity of AD46 antibody remained identical even after subcloning the hybridoma. The immunoreactivity of AD46 with multiple yet unrelated proteins on Western blots, suggests that the epitope is rather conformational than sequence specific in SDS-denaturating conditions. However, a polyclonal antibody against the ATP synthase α-chain strongly labeled NFT of AD while no staining was observed with the NSE antibody or the actin antibody. A staining of mitochondria would have been expected with AD46 or the ATP synthase α-chain antiserum on control brain-tissue sections. Neither AD46 or ATP synthase α-chain antiserum detected mitochondria on brain-tissue section in our conditions, nor NSE antibody or the actin antibody or even with tau antibodies (data not shown). This result is not surprising since tau antibodies only detect tau proteins that accumulate and aggregate in NFT (Buee-Scherrer et al., 1996; Delacourte et al., 1999), whereas normal tau proteins are not detected on control brain-tissue sections. Hence, ATP synthase α-chain cytosolic staining suggests an accumulation of this protein at the immunochemical level, as observed for pathological tau in NFT.

The use of AD46 for immunochemistry study on brain tissue sections of cases of our brain bank (more than 130 cases: 60 controls and 70 AD cases), demonstrated that

**Fig. 4.** ATP synthase α-chain in Alzheimer's disease (AD). (A) The brain-tissue proteins of a control biopsy (Ctrl biopsy), five autopsy controls (Ctrl) and 10 AD patients (Alz) were fractionated using a gradient of Triton X-100 and sodium dodecyl sulfate. One autopsy control and two AD cases (Alz-1 and Alz-2) are shown. The total lane corresponds to the total brain tissue homogenized in Laemmli buffer. The S1–P4 fractions are detailed in material and methods. AD46 staining in the total lane shows the proteins at 42, 47 and 55 kDa with no significant variations between controls and AD patients. Identical pattern of the distribution of the three proteins is observed in control biopsy and control brain-tissue fractions. The 42-kDa protein is detected in all fractions, with a stronger signal in fractions S1, S2 and P4. The 47-kDa protein is only detected in fraction S1 and S2 whereas the 55-kDa protein is detected in fraction S2 to P4. The immunostaining for the 42- and the 47-kDa protein is very similar between controls and AD patients. Conversely, the 55-kDa protein is not detected in S2 and S3 fractions in AD patients when compared with the control immunolabeling. (B) The distribution of the ATP synthase (ATP Σ) α-chain in control (Ctrl) and in AD (Alz) fractioned brain-tissue proteins was investigated using the ATP Σ α-chain antiserum. The ATP Σ α-chain (indicated by an arrow) is detected in control brain protein fractions S2, S3 and P4 whereas the immunostaining is restricted to AD brain protein P4. In parallel, an immunostaining of pathological tau proteins (τ60, τ64, τ69 and τ74) was performed with AD2 antibody on the same protein fractions. The pathological tau proteins were detected in fractions S1, S2 and P4 whereas no labeling was observed in control brain protein fractions. (C) Paired helical filaments were enriched following the procedure described by Goedert et al. (1992). The enrichment is presented for a control (Ctrl) and AD case (Alz). Tau proteins were stained in crude brain-tissue homogenate (total), in 20,000×*g* pellet (20K P), in the sarcosyl 100,000×*g* supernatant (100K S) and in the 100,000×*g* sarcosyl pellet (100K P). Arrowheads indicate normal tau whereas pathological tau (τ60, τ64, τ69) are indicated by arrows. Note that pathological tau are enriched in the sarcosyl-insoluble pellet (100K P lane) in AD. ATP Σ α-chain labeling was performed using the same samples. The ATP Σ α-chain was detected in the sarcosyl pellet in AD tissue but not in the control tissue. (D) Immunoprecipitation (i.p.) with AD46 and ATP Σ α-chain were performed with 27,200×*g* supernatant in control and AD brain tissue (Alz) followed by labeling either with carboxy-terminal tau antibody (TauCt) or with AD2 monoclonal antibody. Pathological tau proteins (indicated by arrows) were pulled down in AD (AD lanes). Note that tau proteins were not detected in control brain tissue following i.p. with AD46 or ATP Σ α-chain antibodies (Ctrl lanes).

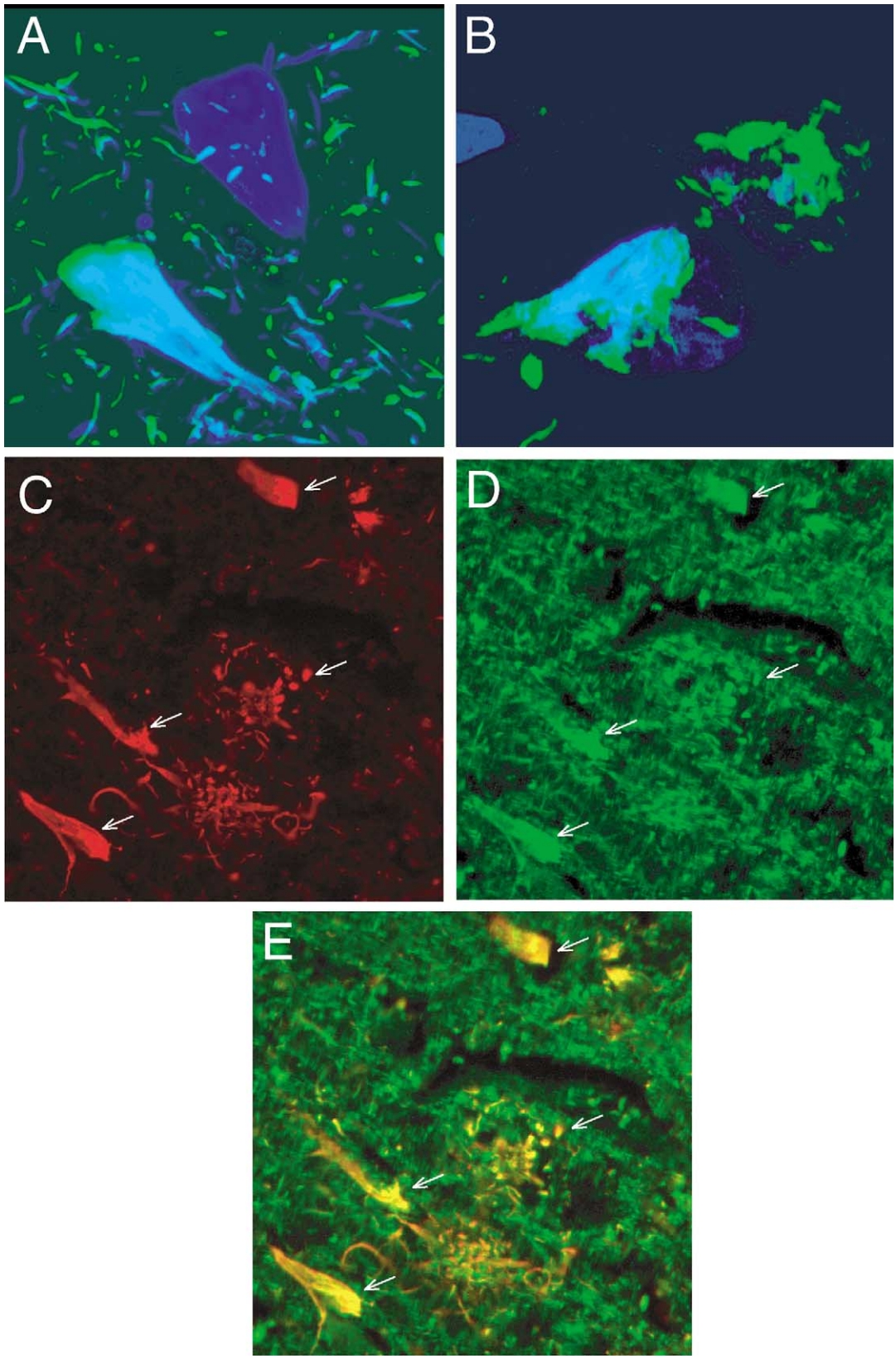


**Fig. 5.**

AD46 reactivity was systematically observed in degenerating neurons of patients affected by tau pathology (Delacourte et al., 1999), even at early stages of tau pathology [stage one according to Delacourte et al. (1999)]. In contrast, AD46 faintly stained neurons and neuropil of control brain tissue. ATP synthase α-chain antiserum and AD46 antibody enabled to visualize selectively NFT in individuals affected by a tau pathology. Therefore, we show here that ATP synthase α-chain cytosolic accumulation and aggregation, alone or associated with tau aggregates, is an additional antigenic component directly related to neurofibrillary degeneration and even at early stages of neurodegeneration (Delacourte et al., 1999).

The ATP synthase α-chain is a mitochondrial regulating subunit of the complex V of oxidative phosphorylation (OXPHOS) and it is localized to the inner membrane of mitochondria. A single gene located on chromosome 18 encodes this regulatory subunit; it is sorted to mitochondria by a signal peptide (first 43 amino acids) and matured to become a constituent of the complex V of OXPHOS (Kagawa and Ohta, 1990; Godbout et al., 1997; Bauer et al., 2000). Our immunofluorescence data suggest a cytosolic localization and accumulation of the ATP synthase α-chain, illustrated by a cytosolic staining of degenerating neurons of AD patients. The maturation of ATP synthase α-chain consists of the cleavage of the first 43 amino acids. The matured form of ATP synthase α-chain is detected in AD, as demonstrated by 2-D gel analysis and the mass-spectrometric identification. The lack of the first 43 amino acids gives a theoretical pI of 8.28 and 8.3 in our experiments, whereas the holoprotein has a theoretical pI of 9.45. Moreover, our results support the association of the matured form of the ATP synthase α-chain with neurofibrillary process in AD. The cytosolic accumulation of ATP synthase α-chain in neurons demonstrates a change of localization suggesting a release by mitochondria or a modification of the maturation of the protein. Moreover, the loss of ATP synthase α-chain in the detergent soluble fractions of AD brain-tissue homogenates shows that the metabolism of this protein is modified in AD.

Mitochondria are involved in programmed cell death (Kroemer and Reed, 2000). It is thought to play a pivotal role in many neurological disorders, including AD and molecular defects have been described (Gabuzda et al., 1994; Cassarino and Bennett, 1999; Beal, 2000; Busciglio et al., 2002). On isolated mitochondria, a lower protein content of the complex V has been described in AD (Schagger and Ohm, 1995). In particular, a lower expression of the β-subunit of ATP synthase has been observed in AD (Chandrasekaran et al., 1997; Kim et al., 2000). However, none of the complex V proteins has been found to co-aggregate with PHF in degenerating neurons of AD, neither other OXPHOS proteins. It was recently suggested that intact complex V is required for apoptosis (Matsuyama et al., 1998). Moreover, the dysfunction of mitochondria has been recently described to alter the APP metabolism, enhancing the intraneuronal accumulation of amyloid β-peptides and enhancing the neuronal vulnerability (Busciglio et al., 2002). Our data, in addition to previous studies, suggest that the function of ATP synthase α-chain is altered in AD degenerating neurons that could participate to the neurodegenerative process of AD. However, it remains to determine how this inner mitochondrial membrane protein accumulates and aggregates in the cytosol of degenerating neurons of AD.

Additional functions of α-chain of ATP synthase have been described as well as extramitochondrial localization in non-neuronal cells. ATP synthase α-chain has been demonstrated to share sequence similarity with chaperones, as the 70-kDa heat-shock cognate (Flores and Cuezva, 1997), and it has been localized to the matrix of rat liver peroxisomes (Cuezva et al., 1990). ATP synthase α-chain has been also observed at the plasma membrane of several tumor cell lines and endothelial cells (Chang et al., 2002; Das et al., 1994; Moser et al., 1999, 2001). In the latter cell type, ATP synthase α-chain was shown to bind plasminogen and its proteolytic-derived fragments as angiostatin (Das et al., 1994; Moser et al., 2001) suggesting extramitochondrial functions of the ATP synthase α-chain, that are in close relationship to peculiar localizations. Interestingly enough, in the brain, plasmin is implicated in the cleavage of APP and the reduction of amyloid β-peptides release. Plasmin was shown to be reduced in AD cases from our brain bank (Ledesma et al., 2000). The cytosolic accumulation of ATP synthase α-chain demonstrated in degenerating neurons of AD support the hypothesis of an altered localization of this protein and consequently the modification of its functions. Therefore, it would be of particular interest to investigate the consequences of the accumulation of the ATP synthase α-chain in the cytosol of *in vitro* models and the consequences regarding the APP and tau metabolism.

In the present study, we demonstrate for the first time a new and additional molecular antigenic component of neurofibrillary degeneration in AD. It consists of the intraneuronal cytosolic accumulation of ATP synthase α-chain that is observed either alone or associated with aggregates of tau proteins of NFT. This phenomenon opens new fields of investigation in the understanding of the implication of mitochondrial protein in neurofibrillary degeneration and

**Fig. 5.** Intraneuronal cytosolic accumulation of ATP synthase α-chain alone or associated with aggregates of pathological tau proteins. Double immunolabeling was performed with a tau antiserum (green channel) and Alzheimer's disease (AD) 46 antibody (blue channel). (A) Colocalisation of tau aggregates and AD46 immunolabeling in the cytosol of a degenerating neuron of AD (white blue staining). AD46 immunostaining is observed independently of tau aggregation (neuron stained in blue). (B) Immunostaining of both tau aggregates and AD46 signal (white blue staining) and intraneuronal aggregates of tau proteins are also observed alone (green staining). (C) Red staining of neurofibrillary tangles, neuropil threads and two neuritic plaques with AD2 antibody. (D) Green staining of AD brain tissue with ATP synthase α-chain. Although the neat serum gives a high background staining, neurofibrillary tangles and degenerating processes in the neuritic plaque are strongly stained. (E) Merged staining of AD2 and ATP synthase α-chain. Colocalized signal are visualized in yellow and are indicated by arrows. The arrows on picture C and D indicated the identical localization of the staining.

could represent a novel target for therapeutic and diagnostic strategies.

*Acknowledgements—This work was supported by INSERM and CNRS. We thank Professor Pierre Formstecher and Maud Collin d'Hooghe from the IMPRT for providing Melanie III software and computer facilities. We are grateful to Daniel Leroy for her helpful advice in immunofluochemistry.*

## REFERENCES

Andersen JS, Mann M (2000) Functional genomics by mass spectrometry. FEBS Lett 480:25–31.

Bauer MF, Hofmann S, Neupert W, Brunner M (2000) Protein translocation into mitochondria: the role of TIM complexes. Trends Cell Biol 10:25–31.

Beal MF (2000) Energetics in the pathogenesis of neurodegenerative diseases. Trends Neurosci 23:298–304.

Braak H, Braak E (1991) Neuropathological staging of Alzheimer-related changes. Acta Neuropathol (Berl) 82:239–259.

Brion JP, Passareiro H, Nunez J, Flament-Durand J (1985) Immunological detection of tau protein in neurofibrillary tangles of Alzheimer's disease. Arch Biol 95:229–235.

Buee L (1999) Cerebrovascular aging. Therapie 54:155–165.

Buee L, Bussiere T, Buee-Scherrer V, Delacourte A, Hof PR (2000) Tau protein isoforms, phosphorylation and role in neurodegenerative disorders. Brain Res Brain Res Rev 33:95–130.

Buee-Scherrer V, Condamines O, Mourton-Gilles C, Jakes R, Goedert M, Pau B, Delacourte A (1996) AD2, a phosphorylation-dependent monoclonal antibody directed against tau proteins found in Alzheimer's disease. Brain Res Mol Brain Res 39:79–88.

Busciglio J, Pelsman A, Wong C, Pigino G, Yuan M, Mori H, Yankner BA (2002) Altered metabolism of the amyloid beta precursor protein is associated with mitochondrial dysfunction in Down's syndrome. Neuron 33:677–688.

Cassarino DS, Bennett JP Jr (1999) An evaluation of the role of mitochondria in neurodegenerative diseases: mitochondrial mutations and oxidative pathology, protective nuclear responses, and cell death in neurodegeneration. Brain Res Brain Res Rev 29:1–25.

Chandrasekaran K, Hatanpaa K, Rapoport SI, Brady DR (1997) Decreased expression of nuclear and mitochondrial DNA-encoded genes of oxidative phosphorylation in association neocortex in Alzheimer disease. Brain Res Mol Brain Res 44:99–104.

Chang SY, Park SG, Kim S, Kang CY (2002) Interaction of the C-terminal domain of p43 and the alpha subunit of ATP synthase: its functional implication in endothelial cell proliferation. J Biol Chem 277:8388–8394.

Cho HS, Hyman BT, Greenberg SM, Rebeck GW (2001) Quantitation of apoE domains in Alzheimer disease brain suggests a role for apoE in Abeta aggregation. J Neuropathol Exp Neurol 60:342–349.

Cuezva JM, Santaren JF, Gonzalez P, Valcarce C, Luis AM, Izquierdo JM (1990) Immunological detection of the mitochondrial F1-ATPase alpha subunit in the matrix of rat liver peroxisomes: a protein involved in organelle biogenesis? FEBS Lett 270:71–75.

Das B, Mondragon MO, Sadeghian M, Hatcher VB, Norin AJ (1994) A novel ligand in lymphocyte-mediated cytotoxicity: expression of the beta subunit of H+ transporting ATP synthase on the surface of tumor cell lines. J Exp Med 180:273–281.

Delacourte A, Defossez A (1986) Alzheimer's disease: tau proteins, the promoting factors of microtubule assembly, are major components of paired helical filaments. J Neurol Sci 76:173–186.

Delacourte A, David JP, Sergeant N, Buee L, Wattez A, Vermersch P, Ghozali F, Fallet-Bianco C, Pasquier F, Lebert F, Petit H, Di Menza C (1999) The biochemical pathway of neurofibrillary degeneration in aging and Alzheimer's disease. Neurology 52:1158–1165.

Delacourte A, Sergeant N, Champain D, Wattez A, Maurage CA, Lebert F, Pasquier F, David JP (2002) Nonoverlapping but synergetic tau and APP pathologies in sporadic Alzheimer's disease. Neurology 59:398–407.

Flores AI, Cuezva JM (1997) Identification of sequence similarity between 60 kDa and 70 kDa molecular chaperones: evidence for a common evolutionary background? Biochem J 322:641–647.

Gabuzda D, Busciglio J, Chen LB, Matsudaira P, Yankner BA (1994) Inhibition of energy metabolism alters the processing of amyloid precursor protein and induces a potentially amyloidogenic derivative. J Biol Chem 269:13623–13628.

Garcia-Sierra F, Hauw JJ, Duyckaerts C, Wischik CM, Luna-Munoz J, Mena R (2000) The extent of neurofibrillary pathology in perforant pathway neurons is the key determinant of dementia in the very old. Acta Neuropathol (Berl) 100:29–35.

Glenner GG, Wong CW (1984) Alzheimer's disease: initial report of the purification and characterization of a novel cerebrovascular amyloid protein. Biochem Biophys Res Commun 120:885–890.

Godbout R, Pandita A, Beatty B, Bie W, Squire JA (1997) Comparative genomic hybridization analysis of Y79 and FISH mapping indicate the amplified human mitochondrial ATP synthase alpha-subunit gene (ATP5A) maps to chromosome 18q12->q21. Cytogenet Cell Genet 77:253–256.

Goedert M, Spillantini MG, Cairns NJ, Crowther RA (1992) Tau proteins of Alzheimer paired helical filaments: abnormal phosphorylation of all six brain isoforms. Neuron 8:159–168.

Greenberg SG, Davies P (1990) A preparation of Alzheimer paired helical filaments that displays distinct tau proteins by polyacrylamide gel electrophoresis. Proc Natl Acad Sci USA 87:5827–5831.

Grundke-Iqbal I, Iqbal K, Tung YC, Quinlan M, Wisniewski HM, Binder LI (1986) Abnormal phosphorylation of the microtubule-associated protein tau (tau) in Alzheimer cytoskeletal pathology. Proc Natl Acad Sci USA 83:4913–4917.

Hensley K, Floyd RA, Zheng NY, Nael R, Robinson KA, Nguyen X, Pye QN, Stewart CA, Geddes J, Markesbery WR, Patel E, Johnson GV, Bing G (1999) p38 kinase is activated in the Alzheimer's disease brain. J Neurochem 72:2053–2058.

Kagawa Y, Ohta S (1990) Regulation of mitochondrial ATP synthesis in mammalian cells by transcriptional control. Int J Biochem 22: 219–229.

Kang J, Lemaire HG, Unterbeck A, Salbaum JM, Masters CL, Grzeschik KH, Multhaup G, Beyreuther K, Muller-Hill B (1987) The precursor of Alzheimer's disease amyloid A4 protein resembles a cell-surface receptor. Nature 325:733–736.

Kim SH, Vlkolinsky R, Cairns N, Lubec G (2000) Decreased levels of complex III core protein 1 and complex V beta chain in brains from patients with Alzheimer's disease and Down syndrome. Cell Mol Life Sci 57:1810–1816.

Kroemer G, Reed JC (2000) Mitochondrial control of cell death. Nat Med 6:513–519.

Laemmli UK (1970) Cleavage of structural proteins during the assembly of the head of bacteriophage T4. Nature 227:680–685.

Ledesma MD, Da Silva JS, Crassaerts K, Delacourte A, De Strooper B, Dotti CG (2000) Brain plasmin enhances APP alpha-cleavage and Abeta degradation and is reduced in Alzheimer's disease brains. EMBO Rep 1:530–535.

Lefebvre-Legendre L, Vaillier J, Benabdelhak H, Velours J, Slonimski PP, di Rago JP (2001) Identification of a nuclear gene (FMC1) required for the assembly/stability of yeast mitochondrial F(1)-ATPase in heat stress conditions. J Biol Chem 276:6789–6796.

Lemoine J, Chirat F, Domon B (1996) Structural analysis of derivatized oligosaccharides using post-source decay matrix-assisted laser desorption/ionization mass spectrometry. J Mass Spectrom 31:908–912.

Matsuyama S, Xu Q, Velours J, Reed JC (1998) The mitochondrial F0F1-ATPase proton pump is required for function of the proapoptotic protein Bax in yeast and mammalian cells. Mol Cell 1:327–336.

Mena R, Edwards PC, Harrington CR, Mukaetova-Ladinska EB, Wischik CM (1996) Staging the pathological assembly of truncated tau

protein into paired helical filaments in Alzheimer's disease. Acta Neuropathol (Berl) 91:633–641.

Moser TL, Stack MS, Asplin I, Enghild JJ, Hojrup P, Everitt L, Hubchak S, Schnaper HW, Pizzo SV (1999) Angiostatin binds ATP synthase on the surface of human endothelial cells. Proc Natl Acad Sci USA 96:2811–2816.

Moser TL, Kenan DJ, Ashley TA, Roy JA, Goodman MD, Misra UK, Cheek DJ, Pizzo SV (2001) Endothelial cell surface F1–F0 ATP synthase is active in ATP synthesis and is inhibited by angiostatin. Proc Natl Acad Sci USA 98:6656–6661.

Nukina N, Ihara Y (1986) One of the antigenic determinants of paired helical filaments is related to tau protein. J Biochem (Tokyo) 99: 1541–1544.

O'Farrell PZ, Goodman HM, O'Farrell PH (1977) High resolution two-dimensional electrophoresis of basic as well as acidic proteins. Cell 12:1133–1141.

Permanne B, Buee L, David JP, Fallet-Bianco C, Di Menza C, Delacourte A (1995) Quantitation of Alzheimer's amyloid peptide and identification of related amyloid proteins by dot-blot immunoassay. Brain Res 685:154–162.

Reig S, Buee-Scherrer V, Mourton-Gilles C, Defossez A, Delacourte A, Beauvillain JC, Mazzuca M (1995) Immunogold labelling of paired helical filaments and amyloid fibrils by specific monoclonal and polyclonal antibodies. Acta Neuropathol (Berl) 90:441–447.

Schagger H, Ohm TG (1995) Human diseases with defects in oxidative phosphorylation: II. F1F0 ATP-synthase defects in Alzheimer disease revealed by blue native polyacrylamide gel electrophoresis. Eur J Biochem 227:916–921.

Sergeant N, David JP, Lefranc D, Vermersch P, Wattez A, Delacourte A (1997) Different distribution of phosphorylated tau protein isoforms in Alzheimer's and Pick's diseases. FEBS Lett 412:578–582.

Sergeant N, Sablonniere B, Schraen-Maschke S, Ghestem A, Maurage CA, Wattez A, Vermersch P, Delacourte A (2001) Dysregulation of human brain microtubule-associated tau mRNA maturation in myotonic dystrophy type 1. Hum Mol Genet 10:2143–2155.

Sergeant N, David JP, Champain D, Ghestem A, Wattez A, Delacourte A (2002) Progressive decrease of APP carboxy-terminal fragments, associated with tau pathology stages, in Alzheimer's disease. J Neurochem 81:663–672.

Vincent IJ, Davies P (1992) A protein kinase associated with paired helical filaments in Alzheimer disease. Proc Natl Acad Sci USA 89:2878–2882.

Wood JG, Mirra SS, Pollock NJ, Binder LI (1986) Neurofibrillary tangles of Alzheimer disease share antigenic determinants with the axonal microtubule-associated protein tau. Proc Natl Acad Sci USA 83:4040–4043.

*(Accepted 16 September 2002)*